RECENT RESULTS ON ^{208}Pb *

K.H. MAIER

Hahn-Meitner-Institut
Glienicker Str. 100, D-14109 Berlin, Germany

(Received December 10, 1996)

Recent measurements of γ transitions in ^{208}Pb provide much new and reliable information. Excited states of ^{208}Pb are well described by one particle–one hole shell model wave functions. These wave functions have been determined for about 50 levels strictly from the experimental data, mainly spectroscopic factors and γ branching ratios. The matrix elements of the residual interaction are calculated from the wave functions by inverting the Schroedinger equation. The resulting residual interaction is presented.

PACS numbers: 21.30. –x, 21.60. Cs, 23.20. Lv, 27.80. +w

1. Introduction

Recently extensive γ-spectroscopic studies have been performed for ^{208}Pb. As ^{208}Pb is neutron rich, it cannot be produced by fusion-evaporation reactions, that are the standard tool of γ-spectroscopy due to their large cross section and selectivity. The new detector systems of many Compton suppressed Ge-detectors have sufficient efficiency and resolution to employ deep inelastic reactions to excite and measure high spin states, although they produce simultaneously 200 nuclei [1, 2]. States above the Yrast line can be populated by direct reactions and their γ-decay studied by particle-γ coincidences; examples are ^{207}Pb(d, p γ)^{208}Pb and ^{209}Bi(t, α γ)^{208}Pb. The γ-decay pattern of the states is highly characteristic and resolves therefore previously unrecognized multiplets. This is crucial for any detailed structure analysis. The spectroscopic factors from transfer reactions give very clear structure information, but are highly misleading if two unresolved states are interpreted as one. Often the selection rules of γ-decay determine also the spin of the states. A complete set of M1- and E2-matrix elements for the

* Presented at the XXXI Zakopane School of Physics, Zakopane, Poland, September 3–11, 1996.

particles and holes relative to the ^{208}Pb core is known [3–5]. The most important elements have been measured, others reliably calculated, as proven by later experiments. Therefore the γ-decay properties, primarily branching ratios, can be used for a quantitative structure analysis. In the following a short overview of the experimental data is presented. Then the derivation of wave functions is shown for the 10^+ states as an example, and finally the matrix elements of the residual interaction are calculated from the inverted Schroedinger equation and discussed.

2. The experimental data

Deep inelastic reactions have been used to populate high spin states in ^{208}Pb. In all cases the beam energy was about 50 MeV above the Coulomb barrier and thick 208Pb targets that stop all reaction products were used. The γ-radiation following these reactions was measured by γ-γ-coincidences using Compton suppressed multi detector Ge-spectrometers. This implies that the reaction mechanism moves from deep inelastic at the surface of the target to quasi elastic reactions when the beam is slowed down to the Coulomb barrier. The stopping time of the reaction products is around 2 to 3 ps; γ-rays emitted during this time are much Doppler broadened and cannot be detected, but any later transitions from stopped nuclei are sharp. Therefore γ-γ-coincidences are then highly selective and allow to extract detailed spectroscopic information, although about 200 nuclei are produced and the spectra are accordingly complex [1, 2] . ^{208}Pb was studied in this way by the reactions of ^{82}Se and ^{64}Ni on ^{208}Pb [1–3, 6]. These measurements extended the Yrast line to the highest possible spin for a 1 particle–1 hole configuration, namely 14^-. Later measurements with a ^{76}Ge beam using the GASP array at Legnaro reached even higher spins and detected the second 11^+ state and more transitions below the 14^- level [7]. Very recent, not yet evaluated, experiments with beams of ^{136}Xe and ^{208}Pb performed at GSI with 5 Ge-cluster detectors and the crystal ball promise still new results on high spin states. The high spin states close to the Yrast line are usually of quite pure and simple structure and give therefore direct information on the shell model interaction, as discussed below.

States above the Yrast line can be populated by direct reactions with light ions. Many excellent experiments have been performed with charged particle spectroscopy [8]. But there are many multiplets of levels, that cannot be resolved in this way. Therefore with the proton pickup reaction ^{209}Bi(t, α γ)^{208}Pb and the neutron transfer ^{207}Pb(d, p γ)^{208}Pb particle-γ-coincidences have been measured [3, 9]. The outgoing particles have been detected with Si-detectors with about 100 keV resolution; this defines the energy of the populated states. The coincident γ-rays, measured with

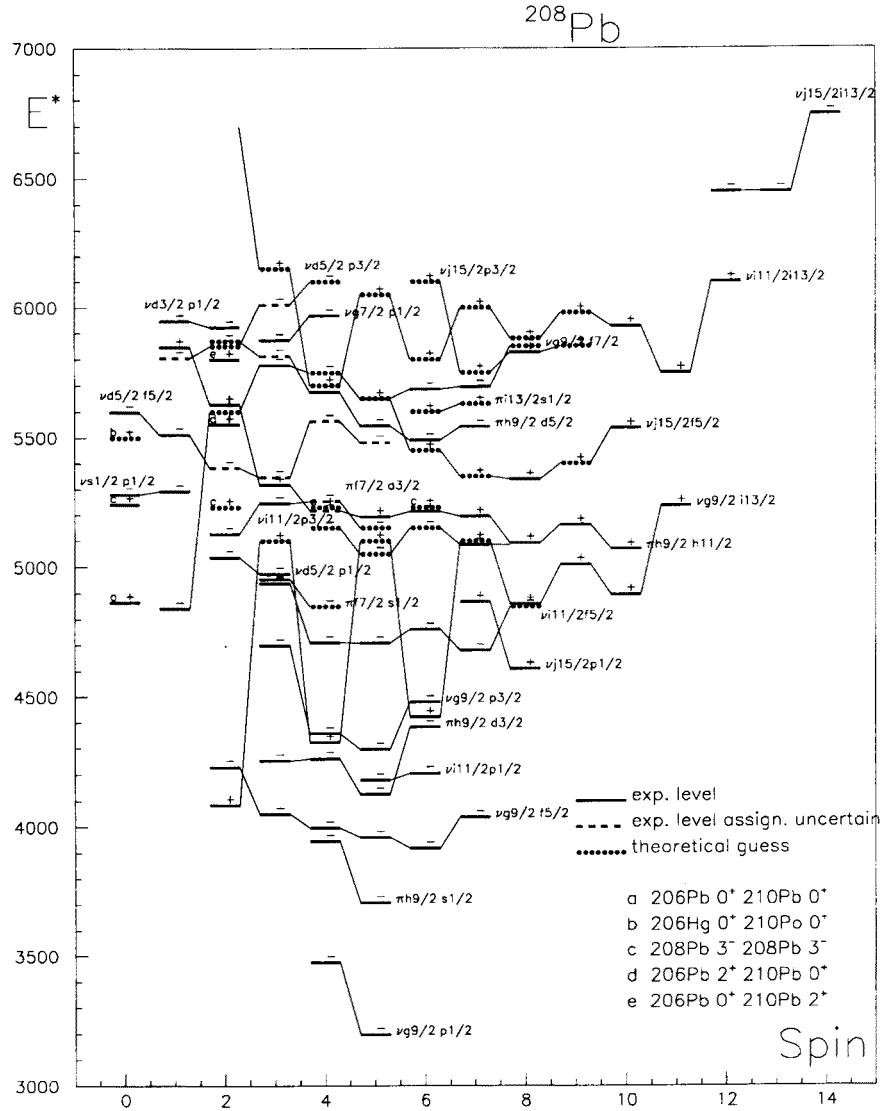

Fig. 1. Schematic presentation of the expected and known states in ^{208}Pb between 3 and 6 MeV excitation energy. The particle–hole configurations that are relevant in this energy range are indicated. Full lines mark experimental levels of known I^{π} with the indicated configuration as main component. Broken lines are also experimental states, but with uncertain I^{π}. Dotted lines mark theoretical guesses by Jan Blomqvist. The few expected two particle–two hole states are also shown.

Ge-detectors, provided however a combined resolution of 2 keV. Therefore now spectroscopic factors could be determined without resolution problems. Equally important many new γ-transitions were found, that also provide detailed information on the structure of the states. While a detailed publication of these experiments is under preparation [10], the results are summarized in Refs. [3, 4]. In particular these references give a complete account of the γ-transitions in ^{208}Pb. Fig. 1 summarizes the information on the states of ^{208}Pb.

3. Derivation of wave functions

Excited states of ^{208}Pb below 6 MeV excitation energy are quite pure single particle–single hole states. The residual interaction is weak and the excitation of another pair takes 3 MeV and can therefore be neglected. The few exceptions, like the pairing vibration states, are not discussed here. As shown for the example of the 10^+ states below, n states of a given I^π are formed by n particle–hole configurations. The wave function of each of theses states is fully described by the n amplitudes of the $p-h$ configurations. Therefore n^2 parameters are to be determined. But the wave functions are orthonormal and therefore the number of parameters is reduced to $n \times (n-1)/2$. M1 transitions can occur between any of the levels with the same I^π. Absolute transition rates are not known, but the measured branching ratios further reduce the number of parameters to $n-1$. The (d, p γ) reaction populates neutron $p-h$ states with the neutron hole in $p_{1/2}$ as in the ground state of ^{207}Pb. The measured spectroscopic factors give the n^2 amplitudes, if such a configuration is present, and the system is already overdetermined. Proton $p-h$ configurations with the particle in $h_{9/2}$ are likewise determined form the ^{209}Bi(t, α) reaction. In addition there are transitions that connect states of different I^π, so that the number of measured parameters often exceeds that of the free parameters.

The derivation of the wave functions is presented here for the example of the four 10+ states, that are composed of the 4 particle–hole configurations indicated in Fig. 3. Other configurations are much higher in energy and can be neglected. Therefore $4 \times 4 = 16$ amplitudes have to be determined, but this number is reduced to 6 free parameters by requiring orthonormality. The γ-decay of the states with $I \geq 10$ is presented in Fig. 2. Fig. 3 depicts the information for the amplitudes of the lowest, isomeric 10^+ state. The spectroscopic factors of the proton pickup reaction give directly the absolute values of the proton configuration for all 4 levels. The strongest component of the lowest state is $\nu g_{9/2} i^{-1}_{13/2}$. The M1-transitions between the 10^+ states proceed primarily from $\pi h_{9/2} h^{-1}_{11/2}$ to $\pi h_{9/2} h^{-1}_{11/2}$

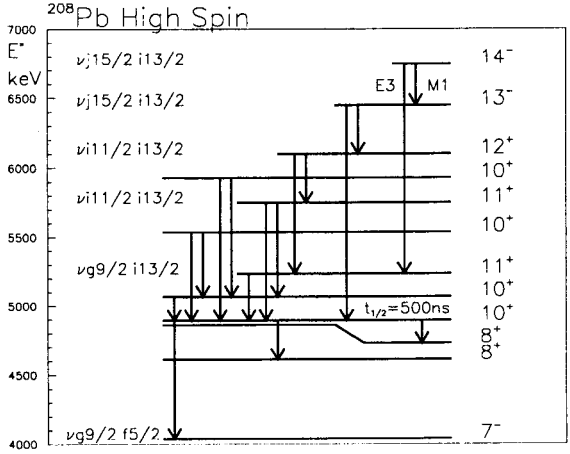

Fig. 2. γ decay of the 10^+ isomer and the higher one particle one hole states in ^{208}Pb.

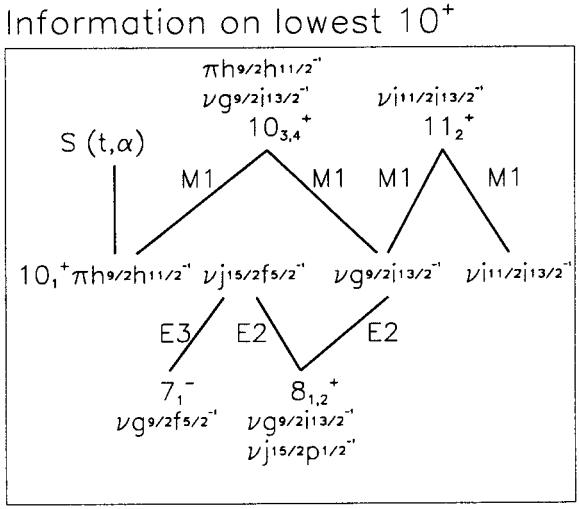

Fig. 3. This figure presents schematically, by which experimental data the amplitudes of the wave function of the lowest 10^+ state are determined.

and from $\nu g_{9/2} i^{-1}_{13/2}$ to $\nu g_{9/2} i^{-1}_{13/2}$. Therefore the measured branching ratios (Fig. 2 and Table II) from the $10^+_{3,4}$ to the $10^+_{1,2}$ connect the amplitudes of these two configurations closely in all 4 levels. The amplitude of the weak $\nu j_{15/2} f^{-1}_{5/2}$ component in the 10^+_1 state is determined by the E3-transition of well known strength to the pure 7^- state. The two E2-transitions to the

two lowest 8^+ states proceed with strong matrix elements from the small $\nu j_{15/2} f^{-1}_{5/2}$ component and weak matrix elements from the large $\nu g_{9/2} i^{-1}_{13/2}$ component. These interfering parts of the transitions connect and determine therefore the amplitudes of these two components. Recently [7] the 11^+_2 state has been found. It is very pure $\nu i_{11/2} i^{-1}_{13/2}$, because no decay to 11^+_1 has been seen. The branching of its γ-decay to $10^+_{1,2}$ is highly sensitive to the amplitude of this configuration in the lowest 10^+ state as shown in Fig. 4. Therefore all 4 amplitudes of the 10^+_1 state are well determined.

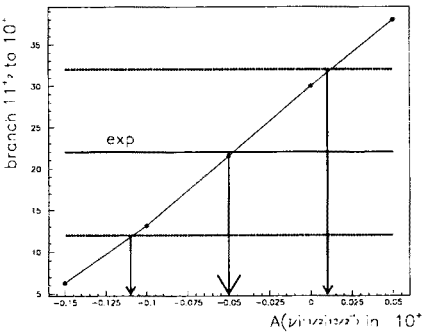

Fig. 4. Branching of the γ decay from the 11^+_2 state to the 10^+_1 state in % as function of the $\nu i_{11/2} i^{-1}_{13/2}$ amplitude of the 10^+_1 state. The experimental branching and the deduced amplitude and the errors are indicated.

Table I presents the wave functions, that have been determined in this way. The γ-decay properties have been calculated from these wave functions (and those of connected states) and are compared with experiment in Table II. It was also possible to extract approximate errors of the amplitudes. The amplitudes in Table I without errors are not well determined, because they are little sensitive to the measured data. Of course γ-transitions always depend on products of amplitudes in the initial and final state, and orthonormality relates all amplitudes for a given spin and parity. Therefore the amplitudes are correlated and a rigorous treatment would require an error matrix. γ-transitions are very sensitive to the signs of the amplitudes as the various transition elements add coherently. For instance, the decay of the 11^+_2 state determines the relative signs of the $\nu g_{9/2} i^{-1}_{13/2}$ and $\nu i_{11/2} i^{-1}_{13/2}$ components in the 10^+ state unambiguously (see Figs. 3 and 4). But no M1- or E2-transition connects the $\pi h_{9/2} h^{-1}_{11/2}$ configuration with any other configuration in our space. Consequently, the sign of the amplitude of this configuration might be changed simultaneously for all states (not only 10^+). In general one has to check carefully how signs are related.

TABLE I

Empirically determined wave functions of the 10^+ states in ^{208}Pb. Amplitudes without errors are not well determined, as they are little sensitive to the experimental data. The absolute values of the amplitudes for the proton configuration as directly given by the spectroscopic factors are also shown.

	10^+ states							
energy[keV]	4895.3		5069.4		5536.6		5928.0	
configuration	amplitude							
$\nu 2g_{9/2}1i^{-1}_{13/2}$	0.79	(17)	0.38	(17)	0.46	(10)	-0.13	(20)
$\pi 1h_{9/2}1h^{-1}_{11/2}$	-0.57	(5)	0.66	(5)	0.36	(5)	-0.33	(5)
exp (t,α γ)	0.58		0.58		0.41		0.41	
$\nu 1j_{15/2}2f^{-1}_{5/2}$	-0.19	(8)	-0.51		0.81		0.21	
$\nu 1i_{11/2}1i^{-1}_{13/2}$	-0.05	(8)	0.41	(25)	0.01		0.91	

TABLE II

γ decay of the four 10^+ and the 11^+_2 level. Branching ratios calculated from the derived wave functions are compared with experiment.

init		final		Λ	E_γ	b_{th}	b_{exp}	err
4895.4	10^+	4610.9	8^+	E2	284.5	79.	83.8	7.4
		4860.9	8^+	E2	34.5	0.04	0.03	0.01
		4037.6	7^-	E3	857.7	21.	16.2	3.
$T_{1/2}$= 0.74E-06s $T_{1/2exp}$=0.500(50)E-06s								
5069.5	10^+	4895.4	10^+	M1	174.1	100.0	100.0	0.0
$T_{1/2}$= 0.12E-11s								
5536.7	10^+	4895.4	10^+	M1	641.3	79.1	81.2	9.1
		5069.5	10^+	M1	467.2	20.5	18.8	4.8
$T_{1/2}$= 0.51E-13s								
5928.3	10^+	4895.4	10^+	M1	1032.9	60.0	64.8	8.2
		5069.5	10^+	M1	858.8	38.3	35.2	12.6
		5536.7	10^+	M1	391.6	1.1		
$T_{1/2}$= 0.16E-13s								
5749.0	11^+	4895.4	10^+	M1	853.6	21.1	22.0	10.0
		5069.5	10^+	M1	679.5	74.0	78.0	10.0
		5069.5	10^+	E2	679.5	2.2		
		5235.6	11^+	M1	513.4	1.4		
$T_{1/2}$= 0.37E-11s								

Wave functions have been determined for about 50 states ranging from spin 2 to 14 in this way. Little configuration mixing was found with a marked difference between states of natural and unnatural parity. The latter usually show just one dominating configuration, while typically two configurations have similar and large amplitudes for natural parity levels.

4. Empirical residual interaction

Usually one regards the Schroedinger equation $H\psi = E\psi$ as an Eigenvalue equation, the Hamiltonian H is known and the wave functions ψ and energies E are calculated from it. The previous analysis however has determined the wave functions, and the energies are directly measured. Therefore the Schroedinger equation can now be inverted and regarded as a system of linear equations to calculate H from E and ψ. The diagonal matrix elements, calculated in this way, are the sum of the single particle and hole energy and the diagonal element of the residual interaction. Single particle energies are taken from experiment, namely the energies of the levels in the nuclei with one particle more or less than ^{208}Pb. Breaking a pair of protons gains the Coulomb pairing energy; this has been taken as 300 keV for all configurations. The remainder of the diagonal elements is then the contribution of the nuclear residual interaction.

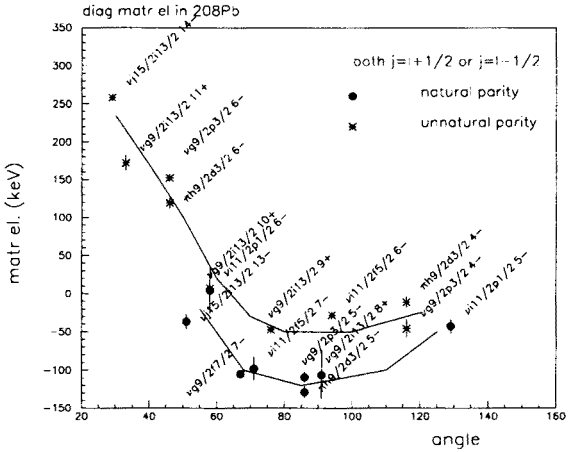

Fig. 5. Diagonal matrix elements of the residual particle–hole interaction in ^{208}Pb determined from experimental data. The abscissa gives the pseudoclassical angle between the spins of the particle and the hole. Configurations and spins are indicated on the points. Both, particle and hole, have either *j=l+1/2* or *j=l-1/2*. Curves to guide the eye are drawn through states with natural ($\pi = (-1)^I$) and unnatural ($\pi = -(-1)^I$) parity.

These matrix elements are shown in Figs. 5–7 as a function of the pseudoclassical angle between the two orbitals. The figures distinguish between the cases, in which the relative direction of spin and orbital angular momentum for particle and hole are the same (both j=l+1/2 or both j=l−1/2) or different (one j=l+1/2 other j=l−1/2). This distinction has been known for

a long time [11]. The second distinction is between natural and unnatural parity of the states. The present analysis shows that the nondiagonal matrix elements of the residual interaction are appreciably stronger for natural parity. The $1^-, 1^+, 2^+$, and 3^- states have been left out, because they likely contain misleading collective admixtures. Unfortunately no "realistic" interactions calculated from the free nucleon–nucleon interaction (see [12]) are yet available for the particle–hole configurations in ^{208}Pb to compare with.

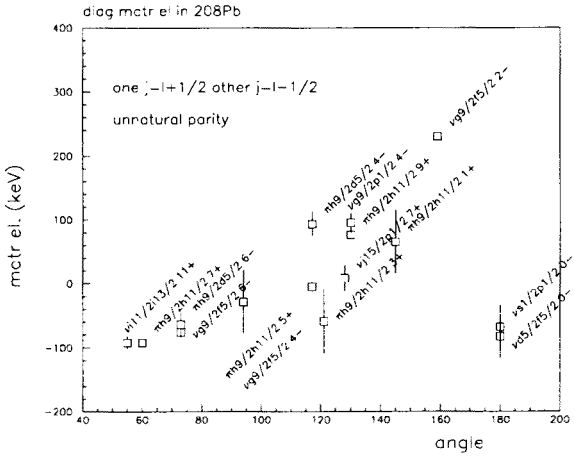

Fig. 6. See Fig. 5. Here configurations, in which the particle has *j=l+1/2* and the hole *j=l-1/2* or vice versa are shown for states of unnatural parity.

Some qualitative features might be mentioned. Figs. 5 and 7 show a clear trend with angle as expected. The planes, in which the particles move, overlap the best at angles close to 0 and 180 deg. and the least at 90 deg. Around 90 deg. the interaction is with about -100 keV attractive. It becomes repulsive ($\sim +250$ keV) at small angles. Values for large angles exist only for the two 0^- states, they are -100 keV. This is surprising for the $\nu d_{5/2} f^-_{5/2} 1$ state, while the definition of the angle is meaningless for the $\nu s_{1/2} p^-_{1/2} 1$ configuration. The pattern suggests an attractive long range interaction, evident around 90 deg., combined with a repulsive short range force that prevails at small angles. The general shift of -300 keV that has been applied for the proton configurations is obviously appropriate, because proton and neutron energies are not distinguished in the figures. The points in Fig. 5 closely follow the two lines, that have been drawn to guide the eye. The indicated trend is a 50 keV shift between the matrix elements for natural and unnatural parity states, while the dependencies on the angle is the same. It is suggested by the data to separate the residual energies for

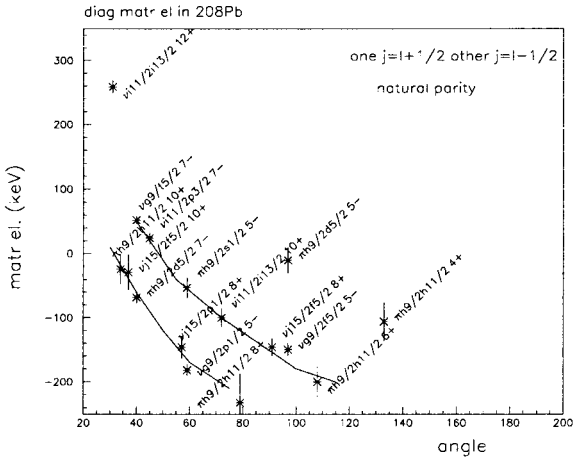

Fig. 7. See Fig. 5. Here configurations, in which the particle has $j=l+1/2$ and the hole $j=l-1/2$ or vice versa are shown for states of natural parity. The curves point out possible trends. It is not understood, that there seem to be two groups of states.

natural parity states and different orientations of l and s into two groups (Fig. 7). But there is no explanation for this division.

5. Conclusions

Many matrix elements of the residual interaction have been determined from experiment. The nondiagonal elements have not been mentioned here, because there is no meaningful way to present them. The diagonal elements show reasonable trends. Much information is also at hand on particle–particle and hole-hole interactions from neighbouring nuclei [8, 13].

Enough and reliable data are available to test theoretical residual interactions. In particular Kuo Brown type [12] calculations of the shell model interaction from the free nucleon interaction are now asked for.

Much more could also be done on the experimental side. Angular distributions of γ rays or measurements of conversion electrons could determine multipolarities and mixing ratios. Inelastic electron scattering is sensitive to completely different aspects of the wave functions. Inelastic proton scattering through analog states could directly determine amplitudes of configurations, that are hardly accessible otherwise.

Because ^{208}Pb and some neighbouring nuclei are stable and therefore available as targets, a wide variety of reactions can be used to study many aspects of nuclear structure experimentally. Simultaneously, the shell model

is a very good theoretical approximation to reality. Therefore, the nuclei around ^{208}Pb offer the possibility for a deeper understanding of the interaction between nucleons inside the nucleus.

I express my sincere thanks to all colleagues that participated in this work from Hahn-Meitner-Institut, Institute of Nuclear Physics, Kraków, and Lawrence Livermore National Laboratory. In particular, N. Roy, M. Schramm and M. Rejmund did much of the work. The data of the Kraków group from the GASP experiment clarified some points. Jan Blomqvist, Stockholm, contributed very valuable advice on many aspects. This work was supported in part by the Polish–German agreement on scientific cooperation (proj. X081.51).

REFERENCES

[1] M. Schramm, H. Grawe, J. Heese, H. Kluge, K.H. Maier, R. Schubart, R. Broda, J. Grębosz, W. Królas, A. Maj, J. Blomqvist, *Z. Phys.* **A344**, 363 (1993).

[2] W. Królas, Deep-inelastic collisions studied by discrete gamma-ray spectroscopy, PhD Thesis, Institute of Nuclear Physics Report No 1738/PL 1996.

[3] M. Schramm, Spektroskopie einfacher Schalenmodellzustände in ^{208}Pb, PhD Thesis, Freie Universität Berlin, 1993, and Report of the Hahn-Meitner-Institut B-508 (1993) ISSN 0944-0305.

[4] M. Rejmund, Nuclear wave functions and residual interaction in ^{208}Pb derived from experimental data, Diploma Thesis, Warsaw University, 1995, unpublished.

[5] K.H. Maier *et al.*, to be published.

[6] W. Królas, R. Broda, J. Grębosz, A. Maj, T. Pawłat, M. Schramm, H. Grawe, J. Heese, H. Kluge, K.H. Maier, R. Schubart, *Acta Phys. Pol.* **B25**, 687 (1994).

[7] R. Broda, J. Wrzesiński, private communication, 1996 and Proceedings of the Conference on Nuclear Structure at the Limits, Argonne 1996 (in print).

[8] M.J. Martin, *Nucl. Data Sheets* **47**, 797 (1986).

[9] N. Roy, K.H. Maier, A. Aprahamian, J.A. Becker, D.J. Decman, E.A. Henry, L.G. Mann, R.A. Meyer, W. Stöffl, G.L. Struble, *Phys. Lett.* **221B**, 6 (1989).

[10] M. Schramm *et al.*, to be published.

[11] M. Moinester, J.P. Schiffer, W.P. Alford, *Phys. Rev.* **179**, 984 (1969).

[12] T.T.C. Kuo, G.E. Brown, *Nucl. Phys.* **85**, 40 (1966).

[13] L.G. Mann, K.H. Maier, A. Aprahamian, J.A. Becker, D.J. Decman, E.A. Henry, R.A. Meyer, N. Roy, W. Stöffl, G.L. Struble, *Phys. Rev.* **C38**, 74 (1988).